ELSEVIER

Physica B 304 (2001) 186–192

PHYSICA B

www.elsevier.com/locate/physb

Optical properties of TiNi, TiCo and TiFe thin films

S.E. Kulkova[a,*], D.V. Valujsky[a], Jai Sam Kim[b], Geunsik Lee[b], Y.M. Koo[b]

[a] *Institute of Strength Physics and Materials Science of the Russian Academy of Sciences, Tomsk State University, pr. Akademichesky 2/1, 634021 Tomsk, Russia*

[b] *Department of Physics, Pohang University of Science and Technology, Pohang 790-784, South Korea*

Received 23 January 2001; received in revised form 20 March 2001

Abstract

The optical conductivity spectra were calculated in B2-TiMe (0 0 1) thin films (Me = Fe,Co,Ni) using the electronic structure obtained by means of the full potential linearized augmented plane wave (FLAPW) method. The changes of optical conductivity in bulk alloys and thin films are analyzed. The difference of the optical conductivity spectrum of the TiNi monoclinic phase from experiment is discussed.

PACS: 71.20.Be; 73.20.At; 78.20.Bh; 78.66.Bz

Keywords: Optical conductivity; Electronic structure; Alloys

1. Introduction

The optical conductivity is a very important characteristic of a material, which can be calculated if its electronic structure is known. The experimental investigations of the optical conductivity spectra ($\sigma(E)$) for TiFe, TiCo and TiNi alloys were performed in [1–4]. Recently, the new measurements of the dielectric function of three 3d titanides were reported in [5]. The newly measured optical spectra for alloys exhibited features similar to previous measurements but the magnitudes of the spectra are different to some degree. A single peak at 1.86 eV was observed for TiFe in [5] while the optical conductivity spectrum given in [2,3] shows a double peak structure at 1.3 and 1.9 eV. Unfortunately, the authors of [5] could not detect the peak at 1.3 eV because experimental spectra were measured in the range 1.5–5.4 eV only but their spectrum for TiFe shows the decrease of $\sigma(E)$ below 1.8 eV and a local minimum around 1.6 eV. In general, the overall shapes of the new spectra are qualitatively similar to the ones of [1–3] but the finer structures observed in the previous works were not seen in [5]. All obtained spectra had broad two-peak features in the visible part of the spectra and for TiFe a minimum at around 2.6 eV separates these peaks.

The structures of the optical conductivity spectra of 3d metal alloys above 1 eV were ascribed in Ref. [1–3] to the interband transitions between the two d-bands separated by the deep minimum near the Fermi level. The structure of the optical spectra in the infrared (IR) region was connected

*Corresponding author. Tel.: +7-3822-286848; fax: +7-3822-259576.

E-mail address: kulkova@ispms.tsc.ru (S.E. Kulkova).

0921-4526/01/$ - see front matter
PII: S0921-4526(01)00553-1

basically with the intraband transitions [1–3]. The sharp decrease of the density of states (DOS) at the Fermi level ($N(E_F)$) in the set of alloys strongly influences the intraband and interband absorptions, especially in TiFe. The strong absorption in IR region in the case of TiNi indicates the presence of the flat bands in the vicinity of the Fermi level and the large value of $N(E_F)$. In general, the optical conductivity spectrum can be a good test for the electronic structure of an alloy.

Several calculations of the optical properties of transition metal alloys were performed in [5–9]. The comparison of the calculated optical spectra for TiFe, TiCo and TiNi [6] with experiment is unsatisfactory. The reason for this discrepancy is connected, first of all with the non-self-consistent band structure calculations. The Green function method was used for the band structure calculations in [6]. Moreover, the interband transition matrix elements were assumed to be constant. The inclusion of the optical transition matrix element in the case of TiNi does not change the result significantly but the finer structure of the spectrum was obtained [3,6]. It is known that the inclusion of optical transition matrix elements in the calculations is very important for an accurate calculation of the optical conductivity spectrum. The detailed investigation of the electronic structure and optical properties for TiNi in B2 and B19′-phases were performed in [7–9]. Unfortunately, the theoretical curves did not reproduce $\sigma(E)$ quite well in B2-TiNi alloy and the change of the optical spectrum during B2–B19′ phase transition in this alloy. It was impossible to understand the appearance of the intensive absorption peak, having an asymmetrical shape, at 0.52–0.80 eV (Fig. 1a) from the calculated electronic structure.

In the paper [5] the calculations of the optical spectra for bulk TiFe–TiCo–TiNi compounds were performed using the linearized-augmented-plane-wave method (LAPW) with the local density approximation (LDA) also. The self-energy correction was used in [5] as done earlier in [7]. It was shown that the calculated optical spectrum of TiFe has 40% and 50% larger magnitude than that for TiCo and TiNi in the region below 2.5 eV. This difference among the spectra of compounds was explained by different transition characteristics from k-points in the Brillouin zone and different bands involved in the transition. It was also shown that the low-energy peak moves towards lower energy from TiNi to TiFe. This fact was in a good agreement with their own experimental result [5] and the results of [1–3]. It is necessary to point out that the calculated $\sigma(E)$ in [7,8] of B2-TiNi has a finer

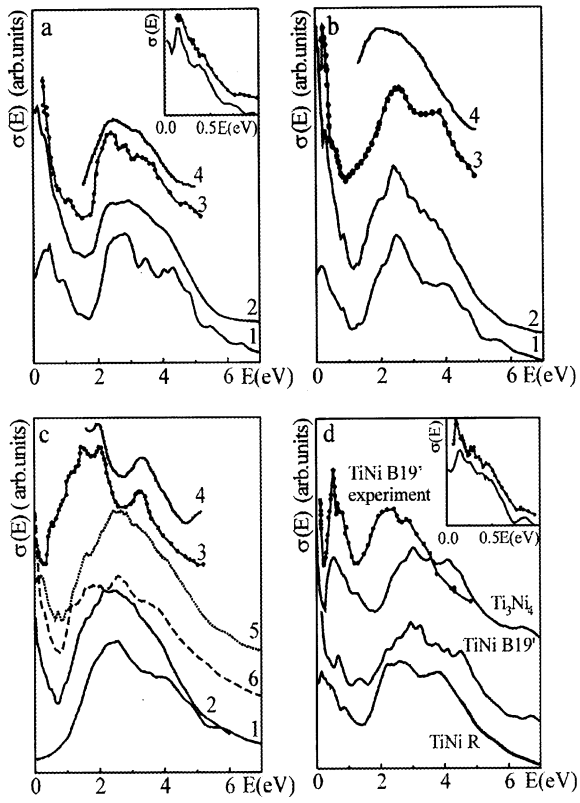

Fig. 1. Optical conductivity $\sigma(E)$ of TiMe (0 0 1) thin films, where Me = Fe, Co, Ni: (a) curve 1—$\sigma(E)$ for bulk B2 TiNi, curve 2—$\sigma(E)$ for Ti-terminated B2 TiNi (0 0 1) film, cuves 3, 4—experiment [1,5], in the inset $\sigma(E)$ for Ti/TiNi is shown in IR region, points—experiment [1]; (b) curve 1—$\sigma(E)$ for bulk B2 TiCo, curve 2—$\sigma(E)$ for Ti-terminated B2 TiCo (0 0 1) film, curve 3,4—experiment [3,5]; (c) curve 1—$\sigma(E)$ for bulk B2 TiFe, curve 2—$\sigma(E)$ for Ti-terminated B2 TiFe (0 0 1) before relaxation, curve 3,4—experiment [3,5], curve 5,6—$\sigma(E)$ for Ti- and Fe-terminated TiFe (0 0 1) film after relaxation process; (d) $\sigma(E)$ for B19′-, R-TiNi, Ti_3Ni_4 and experimental curve for monoclinic B19′-TiNi [1], in the inset the theoretical (solid line) and experimental (points) $\sigma(E)$ [21] for R-TiNi is given in IR-region.

structure in comparison with theoretical result from [5].

The goal of the present paper is to examine the optical properties of 3d titanides for (0 0 1) TiMe thin films and for low-temperature B19′ and R-phase of TiNi. The difference of the optical conductivity spectrum of the monoclinic TiNi phase from the experimental one is discussed.

2. Computational details

Self-consistent band structure calculations of B2-TiMe (0 0 1) surfaces were performed by means of the WIEN implementation of the FLAPW method [10] with LDA for the exchange-correlation potential. We have also parallelized the code for large-scale surface computation [11]. Repeated slabs separated in z-direction by a vacuum region simulated the surface. The thickness of the vacuum region between the slabs corresponding to the three bulk lattice spacings was found to be sufficient for avoiding interactions of Ti(Me) atoms. The wave function within the muffin-tin (MT) spheres were expanded in spherical-harmonics with angular momenta up to $l_{\max}^{\mathrm{wf}} = 10$. Non-spherical contributions to charge density and potential within the MT spheres were considered up to $l_{\max} = 4$. It was shown that a 7-layer TiMe slab represents a good approximation of the (0 0 1) surface. The interlayer distances were optimized with damped Newton dynamics. The band structure was calculated at 72 k-points in the irreducible part of the Brillouin zone (IP BZ) for (0 0 1) surface. More details of the surface calculation are described in our paper that will be published soon. It should be noted that the comparison of local density of states for inner layers with those obtained for bulk TiMe compounds show a good accuracy of the bulk region representation in the film calculation. In the case of bulk compound calculations, the generalized-gradient approximation for the exchange-correlation potential [12] was also used. The electron spectrum of TiNi was calculated at 165 k-points in IP BZ for cubic phase and at 128 and 144 k-points for monoclinic and rhombohedral phases, respectively.

3. Results and discussion

The theoretical optical conductivity spectra for 3d titanides in B2-phase are presented in Figs. 1a–c. Since new experimental spectra [5] did not cover the low-energy region we will compare our calculated spectra with experimental ones reported in [1–3]. Usually the theoretical curves for transition metals and their compounds are displaced by 0.5–1 eV from the experimental ones within LDA. It is known that low-lying exited states near the Fermi energy have reduced energies in comparison with those calculated from ground state potential [13]. The self-energy correction was not included in the present calculations because its influence is obvious. The inclusion of this correction leads to the shift of the calculated $\sigma(E)$ curve but its width and shape do not change significantly. In particular, the self-energy correction for the states was simulated in [7] by shifting each eigenvalue by $0.3(E_n(k) - E_{\mathrm{F}})\, q_{3\mathrm{d}}^{\mathrm{Ni}}$, where $q_{3\mathrm{d}}^{\mathrm{Ni}}$ is the partial local Ni 3d charge in the Ni sphere. The following equation $\sigma_{\mathrm{c}}(E) = 1/(1+\lambda)\sigma_{\mathrm{u}}[E/(1+\lambda)]$, where σ_{c} and σ_{u} are corrected and uncorrected optical conductivity, respectively and λ is fitting parameter, was used in [5]. We did not find significant changes in $\sigma(E)$ within GGA for bulk compounds and therefore LDA was used only in surface calculations. We remind the reader that the surface electronic structure has many sharp peaks in comparison with that of bulk. To simulate the instrumental resolution the Lorentzian lifetime broadening of width 0.2 eV as in [7] was applied to the optical conductivity curves.

As seen from Fig. 1a the curve 2 obtained for Ti-terminated B2 TiNi(0 0 1) film is close to the experimental curve obtained for B2 TiNi bulk compound in [1]. Moreover, it reproduced the experimental peaks well in the low-energy region (inset to Fig. 1a) which we could not obtain previously using the bulk electronic structure (curve 1 in Fig. 1a). Note that the intraband contribution to $\sigma(E)$ is not given in Fig. 1a. Its effect is significant up to 0.5 eV. The calculations for bulk compounds show that the theoretical curves, which represent intraband contribution have no fine structure. Besides the intraband contribution gives rise to $\sigma(E)$ for B2 bulk TiNi

in the above mentioned region and low energy peak in IR does not appear on the total curve. Fig. 2 shows the theoretical curves, which reproduce $\sigma(E)$ for bulk region in the surface calculation for both Ti- and Ni-termination of the film. The calculated $\sigma(E)$ curves are in good agreement with that for bulk B2 TiNi compound. This fact also confirms a good representation of bulk region in 7-layer slab calculation. The optical conductivity for Ni-terminated surface is shown in Fig. 3 (curve 1). This curve is shifted towards E_F and differs significantly from the experimental curve.

As seen in Fig. 1b, the curve 2 obtained for Ti-terminated TiCo (0 0 1) surface is also close to the bulk $\sigma(E)$ (curve 1 in Fig. 1b) in the visible part of spectrum and the sharp increase of $\sigma(E)$ near the Fermi level is observed as on the experimental curve [3]. The minimum of the optical conductivity around 3 eV is less pronounced in the thin film case. The spectra obtained for both Ti- and Co-terminated films show in good resemblance to each other above 2.5 eV where the low-energy peak of $\sigma(E)$ for TiCo is located. The curve for Co-terminated surface is given in Fig. 3 (curve 2). It is also shifted to E_F as in the case of Ni-terminated TiNi (0 0 1) film. It has finer structure in the lower energy range and differs significantly from the bulk curve. $\sigma(E)$ obtained for Fe-terminated TiFe (0 0 1) film (Fig. 3, curve 3) is also shifted towards E_F. It has a peak at 0.5 eV, which appears only as a small shoulder in Ti-terminated TiFe (0 0 1) surface (curve 2 in Fig. 1c). It is necessary to point out that $\sigma(E)$ for Ti-terminated TiFe (0 0 1) surface differs essentially from the theoretical curve for bulk compound and experimental one. It has no minimum between two peaks in the visible part of spectra as in bulk TiFe, but it is more prominent for the Fe-terminated film. The increase of $\sigma(E)$ near the Fermi level in the case of Ti-terminated TiFe (0 0 1) is connected with the shift of E_F from the deep minimum between two main peaks of DOS in the bulk calculation to the antibonding Ti states in the surface calculation. The increase of $N(E_F)$ also takes place in this case. All these features indicate that B2 TiFe (0 0 1) thin film can be unstable in

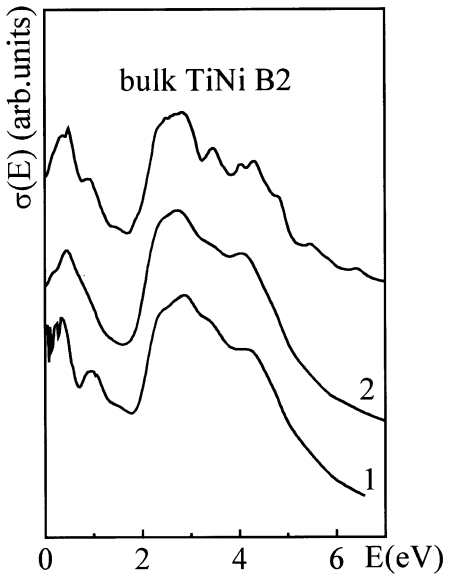

Fig. 2. $\sigma(E)$ for bulk B2-TiNi without intraband contribution, curves 1 and 2 represent $\sigma(E)$ for bulk region in the surface calculation for Ni- and Ti-terminated TiNi (0 0 1) thin films, respectively.

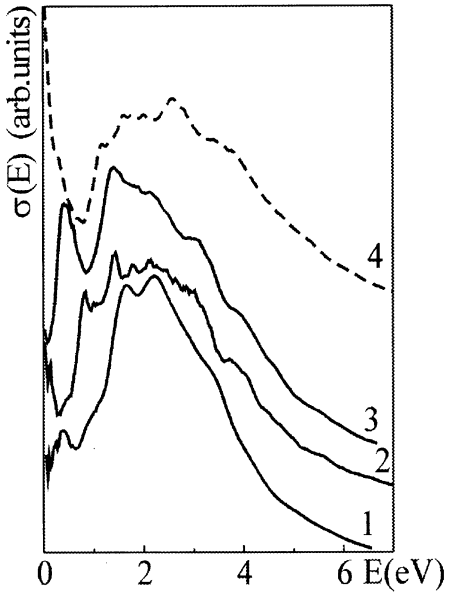

Fig. 3. Optical conductivity $\sigma(E)$ for Me-terminated B2-TiMe (0 0 1) films: curves 1–3—$\sigma(E)$ for Ni-, Co-, Fe-terminated films and curve 4—$\sigma(E)$ for Fe-terminated TiFe (0 0 1) film after relaxation process.

comparison with the bulk compound. It is also necessary to emphasize that the ferromagnetic order is displayed in the case of Fe and Co top layer with a magnetic moment of 2.27 and 0.87 μ_B respectively, whereas Ni in TiNi (0 0 1) has no magnetic moment at all. In general, the optical conductivity spectra for Ti-terminated TiNi and TiCo (0 0 1) thin films are very close to the experimental results obtained for bulk compounds [1,3]. The narrowing of the spectra in comparison with bulk curves is connected with the decrease of the valence bandwidth in the surface calculation.

The result of $\sigma(E)$ calculations can be changed if we take into account the surface relaxation. Within LDA we calculate an inward relaxation of the Fe top layer -25.8% and much smaller relaxation of Ti-top layer -13.9%. Only slight outward relaxation of the subsurface layer (1.5%) was obtained for the both film terminations. The obtained values can be compared with the result for transition metal on an inert substrate. In [14] the large inward relaxation (-30.9%) was predicted for two nonmagnetic monolayers (ML) of Mn on the Cu(0 0 1) substrate but the magnetism affects this value significantly. In [15] the values of relaxation for the first interlayer distance -17.0% and -13.4% were obtained for non magnetic and magnetic 2 ML Co/Cu(0 0 1) systems, respectively. We think that it is necessary to study the more thicker film fixing the two innermost layers at the coordinate of the bulk and in this case only it is possible to correctly estimate the values of the interlayer distances of the top three layers on each side of the slab. Unfortunately the increase of the film thickness leads to an essential increase of the computational expenses.

It was interesting to estimate the influence of the decreasing of the first interlayer distance on the shape of the optical conductivity spectrum. The structure of $\sigma(E)$ for Fe/TiFe film changes more significantly than that for Ti/TiFe (0 0 1) surface. $\sigma(E)$ for Fe/TiFe is given by the dashed line in Fig. 3 (curve 4). You can see the shoulder at 1.2 eV on the theoretical curve as on the experimental one but it shifts in the high-energy region. The curve 5 in Fig. 1c reproduces $\sigma(E)$ for Ti-terminated film after relaxation process. It changes less because the decreasing of the interlayer distance is much smaller in this case. Our results show also that the effect of the surface relaxation on the optical spectrum is less prominent for TiNi among the alloys considered. In addition, the results of calculations for Me-terminated films suggest that the fine structure of the optical conductivity in the low energy region is basically connected with the Me contribution.

It is known [16] that the change of the surface composition depends strongly on the treatment of sample. We suggest that the change of the surface composition can be a reason for the appearance of the sharp peak at 0.5–0.8 eV (Fig. 1d) in the experimental curve for B19′-TiNi [1]. All calculations of $\sigma(E)$ for martensitic monoclinic B19′-TiNi indicate a peak of low intensity in the range where the experiment gives a sharp increase of absorption. This discrepancy with the experiment does not allow us to conclude that the electronic structure of the bulk monoclinic phase was calculated correctly. The four variants of the crystal structure for B19′-TiNi were investigated in [9,17]. Our calculations and results [17] indicate that in the case of the lattice parameters of Kudoh and co-workers [18] the electronic structure changes most significantly from the parent B2-TiNi structure (Fig. 4d) and a dip occurs near the Fermi level (Fig. 4b). Moreover, the crystal structure [18] has the lowest formation energy of the different crystal structures suggested for B19′-TiNi. The appearance of the states in the energy gap typical for B2-TiNi can be seen in Fig. 4b, where the density of states of B19′-TiNi is given. These states may be responsible for the small peak at 0.8 eV, which occurs in all calculations of the optical conductivity for B19′ TiNi [7–9].

It was known that nothing of the kind as in B19′-phase was found during B2-R martensitic transformation. We calculated the electronic structure and $\sigma(E)$ for the pre-martensitic R-phase also. The obtained DOS result is shown in Fig. 4c. It is slightly different from the one obtained in [19] and closer to that of B19′-phase. Note that in both calculations the same lattice parameters from [20] were used. There is no dip near the Fermi level as in B19′-phase and a larger $N(E_F)$ value is obtained.

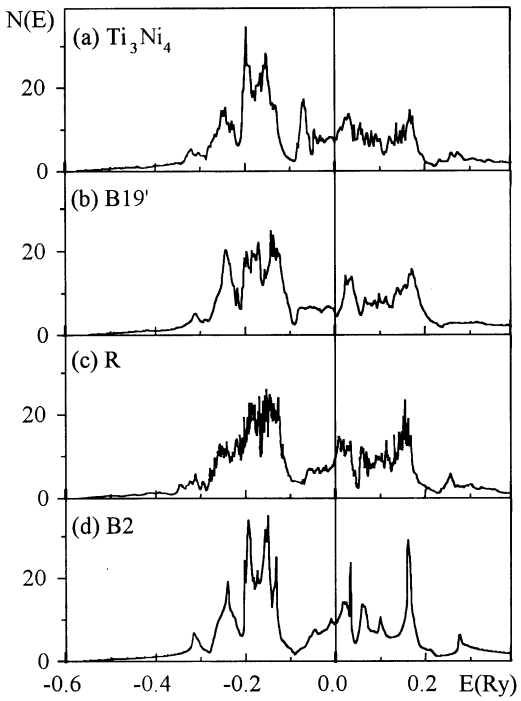

Fig. 4. Total density of states of Ti_3Ni_4 (a) and TiNi in martensitic B19′-phase (b), pre-martenstic R-phase (c) and austenitic B2-phase (d).

In accordance with experimental data [21] we observe only a slight change in the optical conductivity spectra up to 1 eV in comparison with B2-phase. Our result for R-phase is in good agreement with experiment [21], (the inset to Fig. 1d). Unfortunately, the experimental curve for R-phase is given only up to 1 eV in Ref. [21] and it is impossible to compare the theoretical curve with the experiment above 1 eV, where the main peaks of $\sigma(E)$ occurred.

We calculated $\sigma(E)$ for metastable Ti_3Ni_4 phase also. The Ti_3Ni_4 phase having a rhombohedral structure precipates at the early stage of aging. It is interesting that DOS calculation shows sharp increase of $N(E)$ near the Fermi level in this case (Fig. 4a). The optical conductivity spectrum also show a sharp peak in the above-mentioned 0.5–0.8 eV region (see Fig. 1d), where the experimental peak for the martensitic B19′-phase exists. It is very difficult to understand the appearance of the Ti_3Ni_4 precipitation in the bulk compound at the investigated composition in [1] but it is easy to explain the change of the composition and structure at the surface. Our surface calculations for B2 TiNi (0 0 1) show the high chemical reactivity of Ti in comparison with Ni, in good agreement with experiment [22]. In order to understand better the martensitic monoclinic B19′ structure of TiNi a new optical experiment is desirable. It is possible to find the crystal structure of B19′-phase on the basis of a minimization of the total energy. Unfortunately, it needs to be optimized for a large number of parameters. Such kind of calculation remains a very expensive computational task.

4. Conclusion

So the present calculations of the optical conductivity spectra for TiMe (0 0 1) thin films and bulk compounds allow us to conclude:

(i) The optical conductivity spectra obtained with the surface electronic structure for Ti- and Me-terminated TiMe(0 0 1) film differ from those in bulk compound in all the considered 3d titanides. They are more close to bulk for Ti-terminaated TiNi and TiCo (0 0 1) and they are in good agreement with experiments [1,3] especially in the low-energy region.
(ii) The fine structure of $\sigma(E)$ in the low-energy region can be connected with the presence of abundant iron (cobalt, nickel) atoms on the real transition metal surfaces.
(iii) The sharp peak on the experimental curve for B19′ TiNi can be caused by Ni impurities.

Our interpretation agrees well with the strong dependence of low-energy peaks on the concentration observed in [4]. In addition, the electronic structure and optical conductivity for the pre-martensitic R-phase in TiNi were calculated. The obtained result is also in good agreement with experiment [21]. We hope that the present paper will stimulate the experimental investigation of the optical properties for thin films of intermetallic alloy.

Acknowledgements

This work was partly supported by a collaborative program between the Institute of Strength Physics and Materials Science RAS, Tomsk, Russia and the Basic Science Reseach Institute, Pohang University of Science and Technology, Republic of Korea. It was jointly funded by KOSEF-2000 research fund also.

References

[1] I.I. Sasovskaya, S.A. Shabalovskaya, A.I. Lotkov, ZhETF 77 (1979) 2341.
[2] I.I. Sasovskaya, Phys. Met. Metallogr. 50 (1980) 976.
[3] I.I. Sasovskaya, Phys. Met. Metallogr. 69 (1990) 75.
[4] I.I. Sasovskaya, Phys. Status Sol. B 164 (1991) 327.
[5] Joo Yull Rhee, B.N. Harmon, D.W. Lynch, Phys. Rev. B 54 (1996) 17385.
[6] V.E. Egorushkin, N.I. Fedyaynova, in: Alloys of Rare Metals with Special Physical Properties, Nauka, Moscow, 1983, p. 24.
[7] G. Bihlmayer, R. Eibler, A. Neckel, J. Phys. Condens. Matter 5 (1993) 5083.
[8] S.E. Kulkova, V.V. Kalchikhin, J. de Phys. IV. 5 (1995) C8–539.
[9] S.E. Kulkova, D.V. Valujsky, I.Yu. Smolin, Izvestiya VUSov, Fizika. 11 (1999) 43.
[10] P. Blaha, K. Schwarz, J. Luitz, WIEN97, Vienna University of Technology, 1997, 161p (Improved and updated Unix version of the origin copyrighted WIEN-code, which was published by P. Blaha, K. Schwarz, P. Sorantin, S.B. Trickey, Comput. Phys. Commun. 59 (1990) 399).
[11] G. Lee, J.S. Kim, Parallelization of the FLAPW method: MPI implementation. POSTECH internal report.
[12] J.D. Perdew, K. Burke, M. Ernzerhof, Phys. Rev. Lett. 77 (1996) 3865.
[13] J.F. Janak, A.R. Williams, V.L. Moruzzi, Phys. Rev. B 11 (1975) 1522.
[14] M. Eder, J. Haffner, E.G. Moroni, Phys. Rev. B 61 (2000) 11492.
[15] R. Pencheva, M. Scheffler, Phys. Rev. B 61 (2000) 2211.
[16] S.A. Shabalovskaya, J. de Phys. IV. 5 (1995) C8–1199.
[17] M. Sanati, R.C. Albers, F.J. Pinski, Phys. Rev. B 58 (1998) 13590.
[18] M. Kudoh, M. Tokonami, S. Miyazaki, K. Otsuka, Acta Metal. 33 (1985) 2049.
[19] T. Fukuda, T. Kakeshita, H. Houjoh, S. Shiraishi, T. Saburi, Mater. Sci. Eng. A 273–275 (1999) 166.
[20] T. Hara, T. Ohba, K. Otsuka, J. de Phys. IV (1995) C8-641.
[21] I.I. Sasovskaya, V.G. Pushin, Phys. Met. Metallogr. 60 (1985) 879.
[22] V.E. Gunter, Shape-memory effects and its application in medicine, Nauka, Novosibirsk, 1992, p. 741.